Bragg grating spectra in a multimode optical fiber

Changgui Lü (吕昌贵) and Yiping Cui (崔一平)

Advanced Photonics Center, Southeast University, Nanjing 210096

The mode coupling in multimode fiber Bragg gratings (MMFBGs) is analyzed by using the coupled-mode theory. The reflection spectra of MMFBGs excited by one mode and two modes are simulated. The results of the calculation show that MMFBGs have multiple reflection peaks due to the coupling between the same modes in counter-propagating direction and the coupling between the adjacent modes in counter-propagating direction, and the spectra depend on excitation conditions of the bounded modes, such as mode power and mode number.

OCIS codes: 050.1950, 060.2340.

Optical fiber phase gratings formed by ultraviolet irradiation[1] have been developed into a critical component for many applications in fiber-optical communication and sensor systems since the first observation of in-core fiber grating filtering by Hill *et al.* in 1978[2]. Fiber gratings in single-mode optical fibers have been well studied[3]. Recently, Mizunami *et al.* provided experimental reflection spectra of MMFBG and brief explanation from the view of the phase matching condition[4]. However, detailed spectral analysis of MMFBG has not been reported yet. Here we analyze theoretically the spectral characteristics of MMFBG by considering two modes coupling in the gratings.

The fiber grating is an optical diffraction grating. Its effect upon a light wave incident on the grating at an angle θ_1 is shown in Fig. 1. When the propagation constants β_1 and β_2 satisfy the phase-matching condition of the fiber grating: $\beta_2 = \beta_1 + \frac{2\pi}{\Lambda}$, where Λ is the period of the grating, the two corresponding modes couple to each other efficiently.

Here we used the coupled-mode theory[5] to analyze two modes coupling in MMFBG for simplicity. A MMFBG has the structure:

$$n(r,\varphi,z) = \begin{cases} n_0 + \delta n_0(1+\frac{r\cos\varphi}{a})(1+\cos\frac{2\pi}{\Lambda}z), & r \le a \\ n_1, & r > a \end{cases}, \quad (1)$$

where n_0=1.4545, n_1=1.45, δn_0=2.2×10^{-3}, a=4 μm, and Λ=0.535 μm. At the wavelengths of around 1.55 μm, there only exists two bounded core modes LP_{01} and LP_{11} in this fiber. The coupling between these two modes can be described by

$$\begin{aligned}\frac{dA_{01}}{dz} &= iA_{01}K^t_{01-01} + iA_{11}K^t_{11-01}\exp[i(\beta_{11}-\beta_{01})z] \\ &+iB_{01}K^t_{01-01}\exp(-i2\beta_{01}z) \\ &+iB_{11}K^t_{11-01}\exp[-i(\beta_{01}+\beta_{11})z], \end{aligned} \quad (2)$$

$$\begin{aligned}\frac{dB_{01}}{dz} &= -iA_{01}K^t_{01-01}\exp(i2\beta_{01}z) \\ &-iA_{11}K^t_{11-01}\exp[i(\beta_{01}+\beta_{11})z] - iB_{01}K^t_{01-01} \\ &-iB_{11}K^t_{11-01}\exp[-i(\beta_{11}-\beta_{01})z], \end{aligned} \quad (3)$$

$$\begin{aligned}\frac{dA_{11}}{dz} &= iA_{01}K^t_{01-11}\exp[i(\beta_{01}-\beta_{11})z] + iA_{11}K^t_{11-11} \\ &+iB_{01}K^t_{01-11}\exp[-i(\beta_{01}+\beta_{11})z] \\ &+iB_{11}K^t_{11-11}\exp(-i2\beta_{11}z), \end{aligned} \quad (4)$$

$$\begin{aligned}\frac{dB_{11}}{dz} &= -iA_{01}K^t_{01-11}\exp[i(\beta_{01}+\beta_{11})z] \\ &-iA_{11}K^t_{11-11}\exp(i2\beta_{11}z) \\ &-iB_{01}K^t_{01-11}\exp[-i(\beta_{01}-\beta_{11})z] - iB_{11}K^t_{11-11}, \end{aligned} \quad (5)$$

where $A(z)$ and $B(z)$ are slowly varying amplitudes for the transverse mode fields traveling in the $+z$ and $-z$ directions, respectively, K^t is the transverse coupling coefficient. The longitudinal coupling coefficient K^z has been neglected in Eqs. (2)–(5) since K^z is much smaller than K^t for fiber modes. K^t is given by

$$K^t_{vu}(z) = \frac{w}{4}\int_0^{2\pi} d\varphi \int_0^{\infty} r dr \Delta\varepsilon e_v(r,\varphi)\cdot e_u(r,\varphi), \quad (6)$$

where $\Delta\varepsilon$ is the perturbation to the permittivity, e is the field pattern of the corresponding LP mode. For a small index perturbation ($\delta n << n_0$), we have $\Delta\varepsilon \approx 2\varepsilon_0 n_0 \delta n$ approximately. In Eq. (6), the LP modes are assumed to be normalized such that

$$P = \frac{1}{2}\mathrm{Re}\int_0^{2\rho} d\varphi \int_0^{\infty} r dr e^*_u \cdot e_u = 1 \text{ W}, \quad (7)$$

Under the normalization (7), the power carried by each LP mode is equal to $|A_u|^2 + |B_u|^2$.

This is an initial-boundary-value problem, where $A_{01}(0) = \sqrt{C_1}$, $A_{02}(0) = \sqrt{C_2}$, $B_{01}(L) = 0$, and

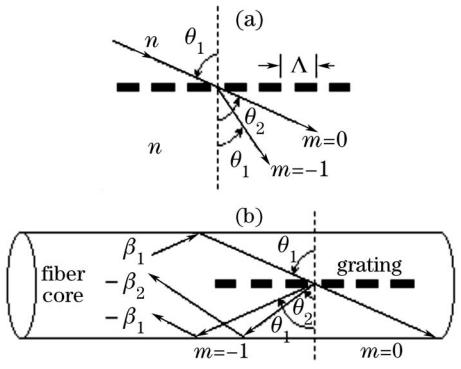

Fig. 1. Illustration of the diffraction of a light by a grating (a) and coupling in MFBG (b).

$B_{11}(L) = 0$, C_1 and C_2 are the initial powers carried by LP_{01} and LP_{11}. To solve these coupled first-order differential equations, the fourth-order Runge-Kutta method is employed here. Comparing Eqs. (2)–(5), we have a common form for these four equations

$$\frac{\mathrm{d}\phi_i(z)}{\mathrm{d}z} = F_i(z, K_{ij}^{\mathrm{t}}(z), \phi_i(z), \phi_j(z)), \tag{8}$$

where $\phi(z)$ stands for the amplitudes for the transverse mode fields in Eqs. (2)–(5), $\phi_j(z)$ stands for all the other $\phi(z)$ except for $\phi_i(z)$. We divide the grating into a number of uniform pieces with length of Δz. Then we can use the fourth-order Runge-Kutta formula based upon Eq. (8). Using the initial set of A_{01}, A_{11}, B_{01} and B_{11}, we can obtain a new set of them. Take the new set as the initial one, repeat the process, and we will get accurate solution to Eqs. (2)–(5). In order that the iterative algorithm converges upon the analytic solution, the set of newly calculated results need to be averaged with the previous one by a weighting factor $0 < f \leq 1$. If the weighting factor is too small, the number of the iterative loops increases. If it is too large, this algorithm will be divergent.

The reflection spectra of the grating described by Eq. (1) are shown in Fig. 2. The grating length is 0.8025 mm. Here we assume that the index change and the mode distribution of LP_{11} are symmetric about the x-axis. Figure 2(a) shows the reflection spectrum of the grating excited by both bounded modes LP_{01} and LP_{11} with equal power. There are three reflection peaks. The left peak and the right peak are due to the coupling between the same modes in counter-propagating direction. The peak in the middle is resultes from the coupling between LP_{01} and LP_{11}. Also shown in Fig. 2(b) is the reflection spectrum of the grating excited only by its fundamental mode LP_{01}. The left peak, which stands for the coupling from LP_{11} to LP_{11}, disappears since there is no LP_{11} mode for the grating to couple to itself. The coupling from LP_{01} to $LP_{11}$and the coupling from LP_{01} to LP_{01} still take place at their own phase-matching wavelengths. In MMF, different modes have different propagation constants. When coupling between two modes satisfies the phase matching condition exactly at some wavelengths, coupling to other modes may not do at those wavelengths. That is also the reason why the grating excited by the fundamental mode has a peak reflection of around 100% while it has a peak reflection of only around 50% is excited by both modes as shown in Fig. 2. When the grating is excited by all the modes, some modes are reflected completely and some modes are reflected partially. Thus a MMFBG excited by fewer modes usually has higher reflectivity than that excited by more modes. If the LP_{11} has the symmetry about y-axis, according to Eq. (6), coupling between LP_{01} and this type of LP_{11} can not occur. However coupling from LP_{01} to LP_{11} with the symmetry to x-axis still happens.

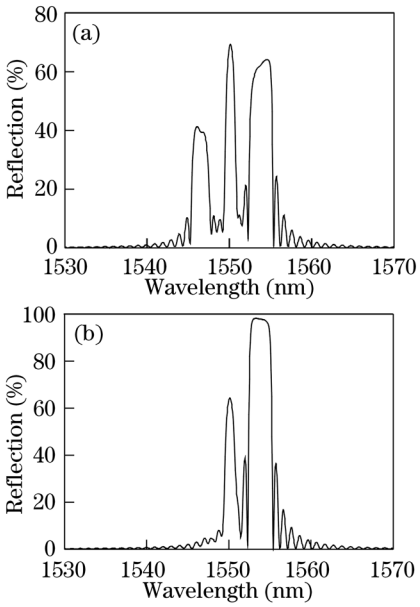

Fig. 2. Reflection spectrum of the grating excited by (a) $LP_{01}$and LP_{11} with equal power, and (b) excited by LP_{01}.

A versatile numerical method has been presented to solve the coupled-mode equations. We simulated two modes coupling by MMFBG and discussed its spectral characteristics. MMFBG shows multiple reflection peaks due to the coupling between the same modes in counter-propagating direction and the coupling between the adjacent modes in counter-propagating direction, and the spectra depend on excitation conditions of the bounded modes, such as mode power and mode number. When a stress exists on MMFBG, the power and the pattern of each mode redistribute. Therefore MMFBG can be used as different types of sensors by detecting the changes of the reflection spectrum. These characteristics are consistent with the experimental results reported in Ref. [4].

This work is supported by Jiangsu Province Natural Science Foundation of China (No. BK2004207) and the National Science Fund for Distinguished Young Scholars of China (No. 60125513). C. Lü's e-mail address is changguilu@seu.edu.cn.

References

1. G. Meltz, W. Morey, and W. H. Glenn, Opt. Lett. **14,** 823 (1989).
2. K. O. Hill, Y. Fujii, D. C. Johnson, and B. S. Kawasaki, Appl. Phys. Lett. **32,** 647 (1978).
3. T. Erdogan, J. lightwave Technol. **15,** 1277 (1997).
4. T. Mizunami, T. V. Djambova, T. Niiho, and S. Gupta, J. Lightwave Technol. **18,** 230 (2000).
5. A. Yariv, IEEE J. Quantum Electron. **9,** 919 (1973).